Biophysical Journal, Volume *112*

Supplemental Information

Live-Cell Super-resolution Reveals F-Actin and Plasma Membrane Dynamics at the T Cell Synapse

George W. Ashdown, Garth L. Burn, David J. Williamson, Elvis Pandžić, Ruby Peters, Michael Holden, Helge Ewers, Lin Shao, Paul W. Wiseman, and Dylan M. Owen

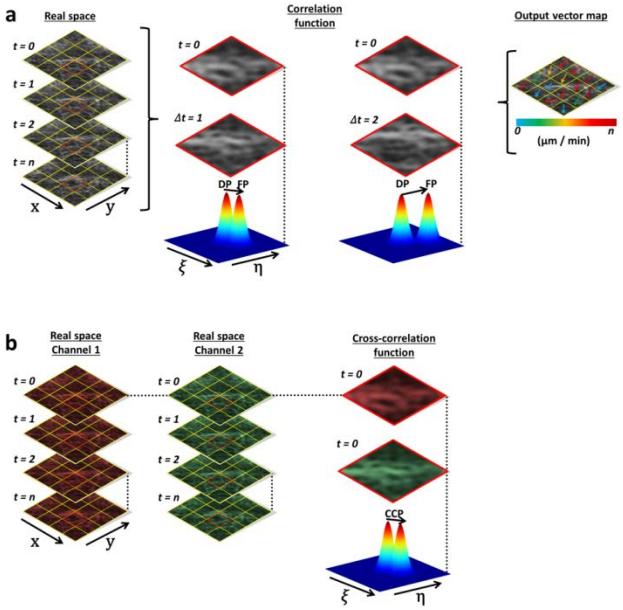

Supplementary Figure 1 Spatio-temporal image correlation and cross spectroscopy (STICS/STICCS) principles. a) By correlating intensity fluctuations in real space as fluorescently labelled molecules move within a subregion of interest through time (red ROI), a correlation function is generated, at zero time lag (t = 0) a peak distribution will be generated at the centre of the function. By correlating t0 with multiple time lags (centre images) any net flow will appear as a second flowing peak distribution (FP), while diffusive (DP) populations remain at the centre of the function. By fitting the translating correlation peak with a function through consecutive time lags, the peak centroid can be tracked to determine the velocity, which can be visualised as a vector map (right), where speed is indicated by the vector colour. b) By cross-correlating two-channel data it is possible to establish any correlation between two fluorescent populations which undergo co-transportation. Here each dataset is autocorrelated as above but also correlated with the other channel, producing a cross-correlation peak (CCP) which can again be visualised as a vector output.

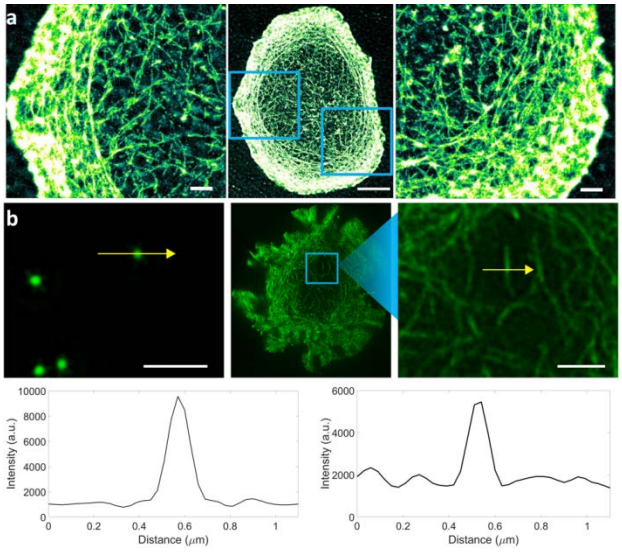

Supplementary Figure 2 Characterisation and resolution capabilities of fixed and live-cell super-resolution methods. a) IRIS localisation microscopy of F-actin network at the T cell immunological synapse. Using an Atto-655 molecule dye tagged to the peptide LifeAct at nanomolar concentrations, a sparse population of actin molecules were labelled. As binding is transient, this allows an SMLM image to be constructed over time. Here, a Jurkat T cell has formed an immunological synapse after contact with a stimulatory αCD3 and αCD28 coated coverslip before being fixed. Centre scale bar = 5 µm. ROI scale bars = 1 µm. b) TIRF-structured illumination microscopy (SIM) resolution characterisation. Reconstructed TIRF-SIM images of 100 nm fluorescent beads resting on a coverslip (left) and Jurkat T cells stimulated as described in a). To test the resolution capability of the SIM system the FWHM of a single fluorescent bead and an actin

fibre within a cell were measured after reconstruction. FWHM profiles of the N-SIM system gave resolutions of 120 nm for the bead (bottom left) and an average of 100.1 ± 11.0 nm for actin fibres (n = 10) (bottom right), while the custom built system gave a FWHM measurement of 98.6 ± 12.4 nm (n = 10) for the green channel and 111.7 ± 15.6 nm (n = 10) for the red channel. Scale bars = 1 µm.

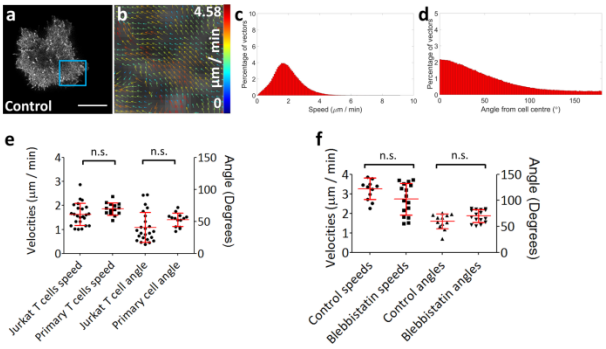

Supplementary Figure 3 a) Comparison of Jurkat E6.1 cell line and Primary Human T cells. F-actin speeds labelled with LifeAct-GFP is not significantly different between Jurkat T cells (n = 24) and primary human T cells (n = 14) when imaged and analysed with STICS under the same conditions (p = 0.098) and b) comparison of Jurkat T cell actin speeds for control versus blebbistatin conditions with cells expressing LifeAct-GFP (p = 0.16, n = 7) or GFP-actin (p = 0.91, n = 8) *a) TIRF-SIM image of a primary human T cell expressing LifeAct-GFP, forming a synapse against a stimulatory coverslip. b) STICS analysis generates vectors which are represented as histograms for c) speed and d) directionality quantification e) F-actin labelled with LifeAct-GFP exhibited non-significant speeds and directionality between Jurkat T cells (n = 24) and primary human T cells (n = 14) when imaged and analysed with STICS under the same conditions. (p = 0.098 and p = 0.08). Mean speed 1.86 ± 0.26 angle 54.9% retrograde. f) Blebbistatin treatments (p = 0.06 and 0.0525), n = 12 and 16.*

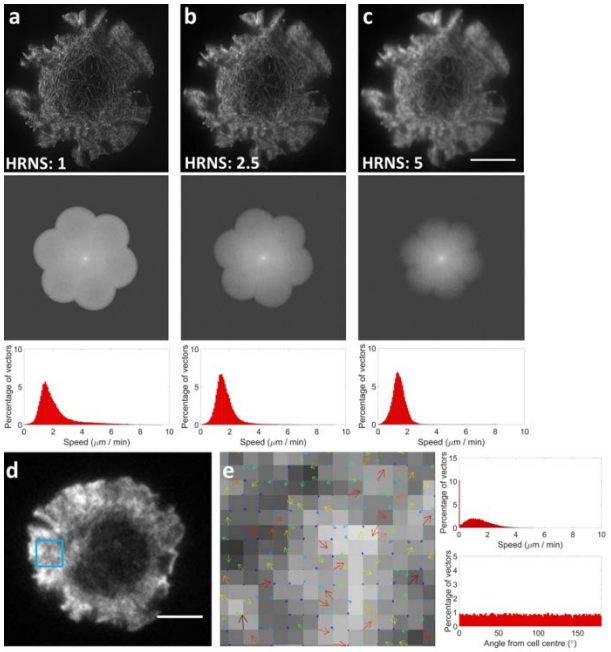

Supplementary Figure 4 STICS is insensitive to spatial filtering. High resolution noise suppression (HRNS) filtering was applied during reconstruction, followed by STICS analysis. After HRNS values of a) 1, b) 2.5, and c) 5, velocity averages were found to be a) 1.97 ± 0.64, b) 1.60 ± 0.26 (p=0.27 relative to control) and c) 1.39 ± 0.16 µm / min (p=0.09 relative to control) respectively (n = 5). D) Standard TIRF imaging of a Jurkat T cell forming a synapse against a coverslip, after STICS analysis of subregion sizes matched to the TIRF-SIM datasets E) it was shown directionality is scrambled. 5 µm scale bars.

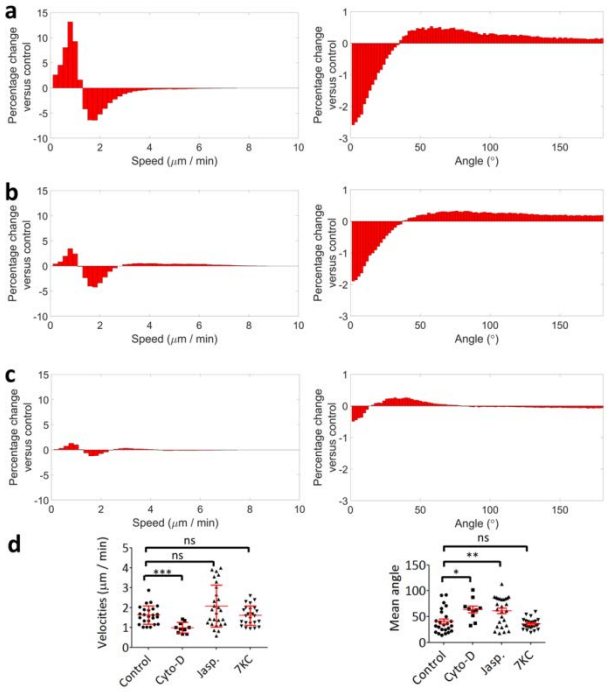

Supplementary Figure 5 Characterisation of F-actin flow in drug treated T cells compared with control conditions. Vector distribution differences of cellular F-actin after drug treatments when compared with control cells. Positive (negative) x-axis values represent bins where the drug treatment cells exhibit greater (lower) numbers of vectors. Cytochalasin-D treated cells (a) have a significant shift towards slower moving vectors (exhibiting a positive or leptokurtic distribution) and have less retrograde directionality when compared with control cells. Jasplakinolide treated cells (b) exhibit a spread distribution (platykurtic) of vector speeds compared with control cells, with vectors populating slower and faster velocities, there is also a similar disruption of directionality. Through disruption of membrane lipid order with the addition of methyl-β cyclodextrin and 7-ketocholesterol (c) a less dramatic but similar platykurtic distribution was observed for vector speeds and directionality was also disrupted but to a lesser extent than actin modulating drugs. d) Scatterplots of mean cell velocities (left) and angles (right) for different drug treatments. Compared to control cells, cytochalasin-D treated cells had significantly slower ($p < 0.001$) average speeds. For directionality, the actin-modulating cytochalain-D increased the mean angle significantly ($p = 0.01$), as did jasplakinolide ($p = 0.008$) indicating polymerization drives retrograde flow order. The disruption of membrane order had no significant effect on the speed or directionality of cell means ($p = 0.88$ and 0.32).

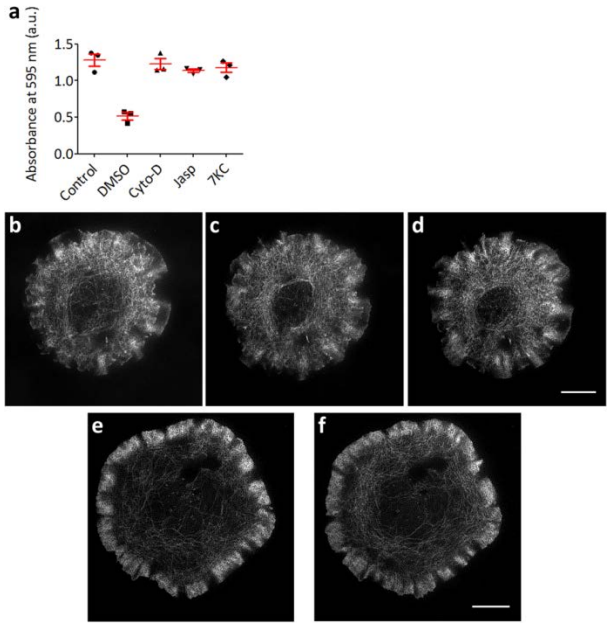

Supplementary Figure 6 MTT cell viability of drug treatments. MTT cell viability of drug treatments. Primary human T cells were incubated under different reagent conditions for 1 hr to assess the viability of the drug treatment concentrations used during imaging. When cell viability is low absorbance decreases. Cells were seeded at 5x 10^6 / 100 µL, data shown from 3 experiments. b) Jurkat T cells were imaged for 1 minute before capturing a single frame 1 minute (c) and 5 minutes (d) post time-course acquisition. These are compared to Jurkat T cells where a single frame was taken before (e) and after (f) a 1 minute interval without imaging.

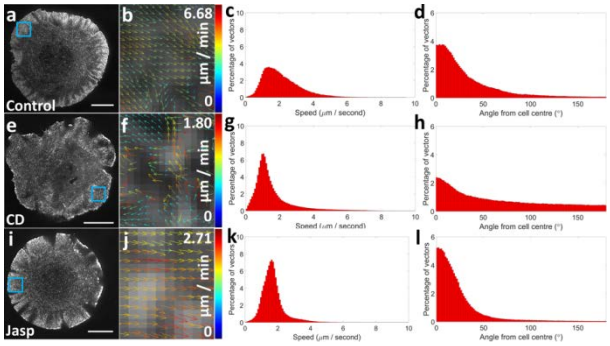

Supplementary Figure 7 MTT cell viability of drug treatments. MTT cell viability of drug treatments. Primary human T cells were incubated under different reagent conditions for 1 hr to assess the viability of the drug treatment concentrations used during imaging. When cell viability is low absorbance decreases. Cells were seeded at 5x 10^6 / 100 µL, data shown from 3 experiments. b) Jurkat T cells were imaged for 1 minute before capturing a single frame 1 minute (c) and 5 minutes (d) post time-course acquisition. These are compared to Jurkat T cells where a single frame was taken before (e) and after (f) a 1 minute interval without imaging.

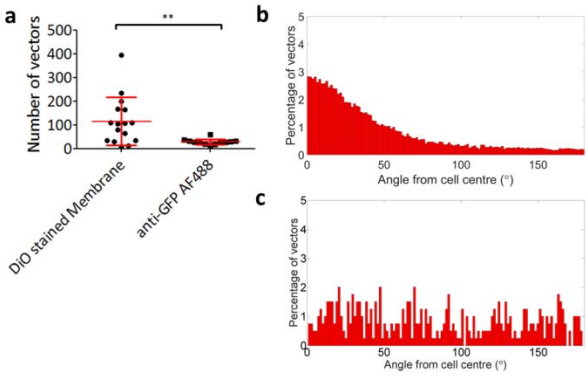

Supplementary Figure 8 STICS of immobile fluorophores bound to glass. Anti-body conjugated fluorophores coating glass coverslips were imaged using TIRF-SIM, absolute number of vectors for a 3 x 3 µm region after STICS analysis is shown (a) along with the directionality histograms for (b) the labelled plasma membrane at peripheral regions of the T cell synapse and (c) the static plate-bound fluorophores. Average numbers of vectors per 3 x 3 µm region were 115.3 and 28.42 respectively.

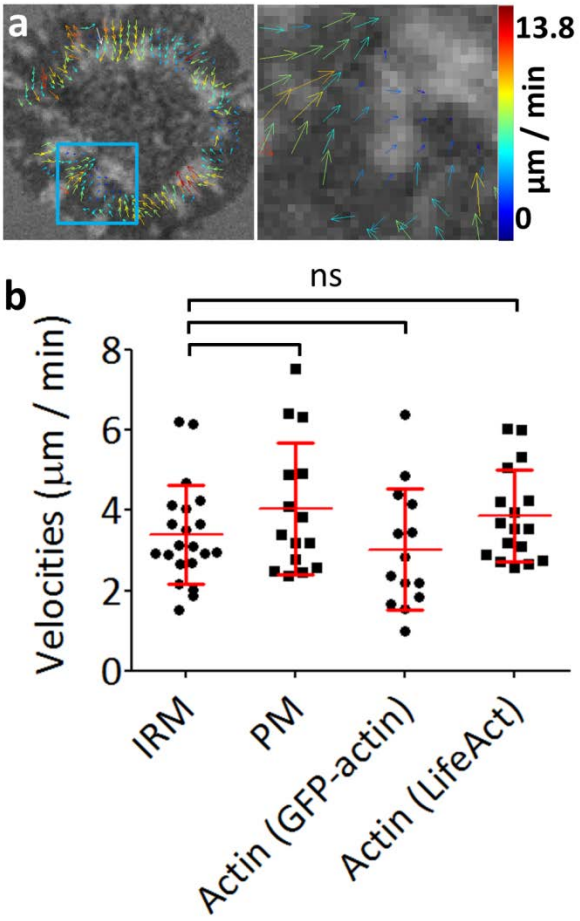

Supplementary Figure 9 STICS of interference reflection microscopy (IRM) data. IRM image of a Jurkat T cell (a) forming a synapse on a stimulatory coverslip (see methods), darker intensities indicate cell body is closer to the coverslip compared with lighter intensities which indicate areas of the cell further from the coverslip. Lighter peripheral patches indicate ruffling of the cell membrane. Comparison of IRM data flow speeds quantified by STICS analysis (b) reveals these ruffles follow a similar direction and speed to the actin and plasma membrane (PM) data taken 3-5 minutes after synapse formation. Mean velocities: IRM 3.39 ± 1.23, n = 21; PM 4.04 ± 1.65, n = 15; GFP-actin 3.02 ± 1.51, n = 14; LifeAct-GFP 3.87 ± 1.08, n = 17.

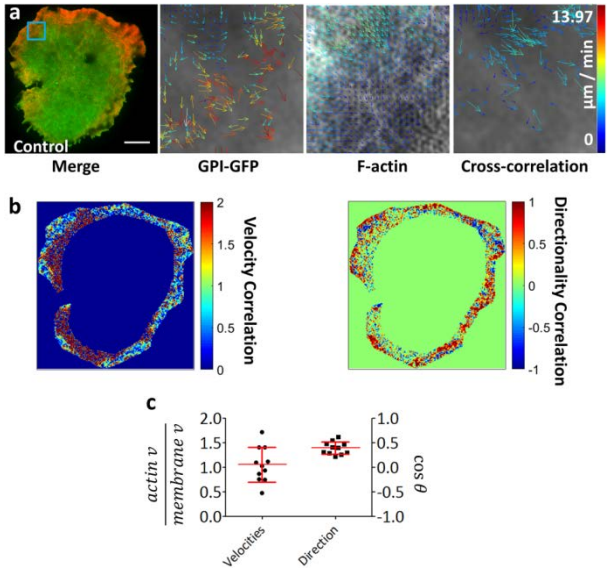

Supplementary Figure 10 Correlation analysis of GPI-GFP and LifeAct mCherry expressing cells. Images in a) show the ordered-residing membrane marker GPI-GFP alongside LifeAct-mCherry with b) showing an average correlated velocity of 1.05 ± 0.35, and correlated directionality 0.39 ± 0.13, n = 11.

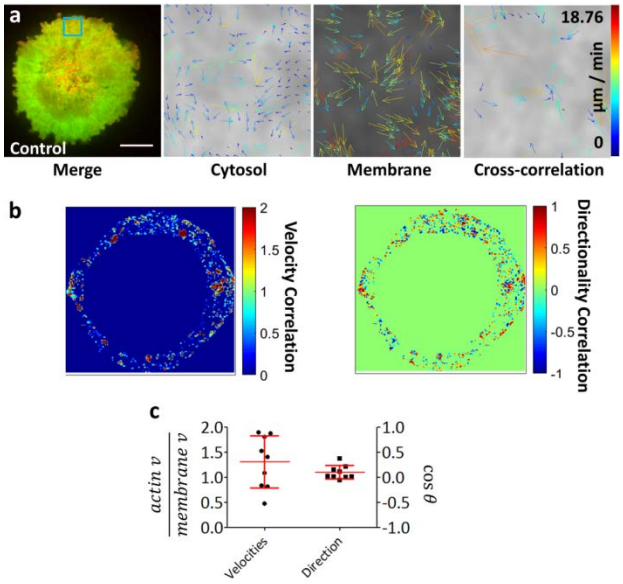

Supplementary Figure 11 Correlative analysis of two non-correlated flowing populations. To demonstrate a negative control we imaged and analysed cells expressing cytosolic-GFP and the membrane dye DiI, showing results of two flows which should not be correlated in a) where average correlated velocity is 1.31 ± 0.52, and correlated directionality is 0.10 ± 0.13, n = 9.

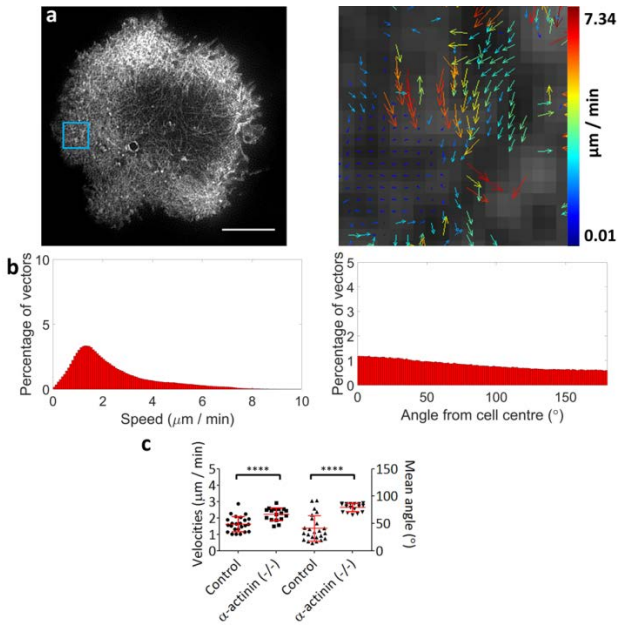

Supplementary Figure 12 Image correlation of the actin cortex by TIRF-SIM and STICS analysis in Jurkat T cell forming immunological synapse after α-actinin CRISPR knockout. A) Image and quantification of α-actinin knockout cells, actin labelled with LifeAct-GFP, and imaged 5 mins after contact with an antibody coated coverslip. Scale bar = 5 µm. B) Histograms show the normalised speed within the dSMAC (left) and directionality (right). C) Scatterplots of individual cell means for actin flow velocity (2.23 ± 0.39 µm / min) and flow directionality (79.4 ± 7.5 °). n = 17. **** = p < 0.0001.

Supplementary Video Captions

Supplementary Video 1. TIRF-SIM showing a Jurkat T cell forming an immunological synapse on a stimulatory coverslip. F-actin is labelled by the actin binding peptide LifeAct-GFP. Scale Bar = 5 µm.

Supplementary Video 2. TIRF-SIM showing a Jurkat T cell forming an immunological synapse on a stimulatory coverslip. Cell is labelled with DiO membrane dye. Scale Bar = 5 µm.

Supplementary Video 3. Interference reflection microscopy of Jurkat T cell forming an immunological synapse on a stimulatory coverslip. Lighter areas indicate cell components further from the coverslip, darker areas closer to the coverslip. Scale Bar = 5 µm.

Supplementary Video 4. Two-channel TIRF-SIM visualising F-actin (left) and the membrane dye DiI (right). Scale Bar = 5 µm.

Supplementary Video 5. Two-channel TIRF-SIM visualising a Jurkat T cells forming an immunological synapse. F-actin (left) is labelled with LifeAct-GFP and the PM (right) is labelled with GPI-GFP. Scale Bar = 5 µm.

Supplementary Video 6. Two-channel TIRF-SIM visualising a Jurkat T cells forming an immunological synapse. F-actin (left) is labelled with LifeAct-GFP and α-actinin (right) is labelled with mCherry. Scale Bar = 5 µm.

Supplementary Video 7. TIRF-SIM showing an α-actinin CRISPR knockout Jurkat T cell forming an immunological synapse on a stimulatory coverslip. F-actin is labelled by the actin binding peptide LifeAct-GFP. Scale Bar = 5 µm.

Supplementary Video 8. TIRF-SIM showing an α-actinin CRISPR knockout Jurkat T cell forming an immunological synapse on a stimulatory coverslip. Cell is labelled with DiO membrane dye. Scale Bar = 5 µm.